ACS Photonics

Article

pubs.acs.org/journal/apchd5

Strong Chiroptical Activities in Gold Nanorod Dimers Assembled Using DNA Origami Templates

Zhong Chen,[†,‡] Xiang Lan,[†,‡] Yu-Che Chiu,[§,‡] Xuxing Lu,[†] Weihai Ni,*[,†] Hanwei Gao,*[,§] and Qiangbin Wang*[,†]

[†]Key Laboratory of Nano-Bio Interface, Division of Nanobiomedicine and *i*-Lab, Suzhou Institute of Nano-Tech and Nano-Bionics, Chinese Academy of Sciences, Suzhou 215123, People's Republic of China

[§]Department of Physics, Florida State University, Tallahassee, Florida 32306, United States

Supporting Information

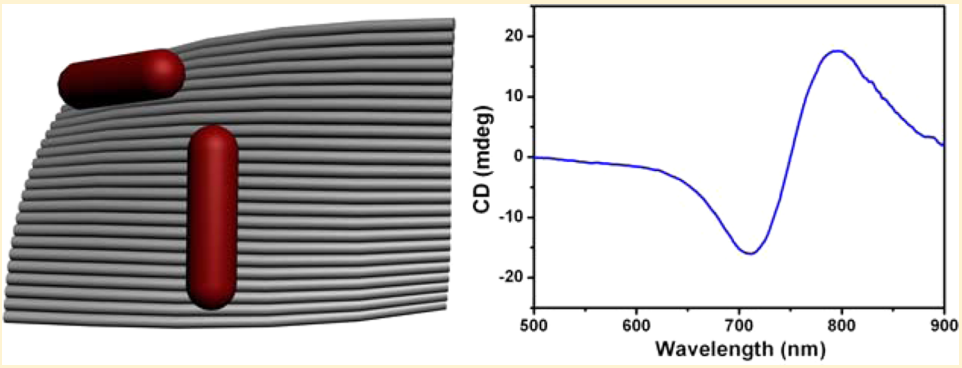

ABSTRACT: Asymmetric three-dimensional (3D) nanoarchitectures that cannot coincide with their mirrored-symmetric counterparts are known as chiral objects. Numerous studies have focused on chiral plasmonic nanoarchitectures created intentionally with 3D asymmetric configurations, whose plasmonic chirality is promising for various nanoplasmonic and nanophotonic applications. Here, we show that gold nanorod (AuNR) plasmonic nanoarchitectures assembled on a soft 2D DNA origami template, which was often simplified to be a rigid rectangle, can exhibit strong chiroptical activities. The slight flexibility of the origami templates was found to play a critical role in inducing the plasmonic chirality of the assembled nanoarchitectures. Our study set a new example of reflecting the native conformation of nanostructures using chiral spectroscopy and can inspire the exploration of the softness of DNA templates for the future design of assembled chiral nanoarchitectures.

KEYWORDS: *chiral nanostructures, DNA origami, plasmonic structures, three-dimensional structure, chiroptical activities*

Chiral plasmonic nanoarchitectures have shown great potentials as building blocks for negative index materials,[1,2] broadband circular polarizers,[3,4] and label-free biosensing and structural characterization of biomaterials.[5,6] The advantages of such metal nanoarchitectures originate in their surface plasmon resonances with strong optical absorption, which can enhance the optical activity significantly.[7−9] Furthermore, the handedness, wavelength, and intensity of the plasmonic chirality can be rationally tuned by simply tailoring the geometry of the nanostructured components.[10−13]

Recently, DNA origami has proved to be a versatile template for controlled assembly of noble metal nanoparticles, allowing the creation of well-defined plasmonic chiral nanostructures. For instances, tubular origami that displays helical arrangement of anchor sites enables organizing of three-dimensional (3D) gold nanoparticle (AuNP) chiral plasmonic helices.[14] Instead of 3D DNA origami, a two-dimensional (2D) rectangular DNA origami has been used to construct 3D chiral plasmonic structures by precisely positioning AuNPs on its up and bottom side, respectively, forming 3D asymmetric AuNP chiral tetramers.[15] One of our recent efforts further extended this facile strategy to obtain complex 3D gold nanorod (AuNR) dimer structures with tunable chiroptical activities by rationally designing the locations of AuNRs on both sides of a 2D rectangular DNA origami.[16]

So far, most of the DNA-guided plasmonic chiral nanomaterials were fabricated intentionally with precise 3D structures. In fact, owing to the flexibility of the DNA molecules, the DNA origami still maintains the nature of soft materials, and exhibits dynamic and Brownian motion in liquid, which will certainly lead to the deformation of the assembled nanostructures. However, the DNA origami used as template for directing the assembly of nanostructures is often treated as rigid and ideal as the designed model. For example, DNA origami has been widely treated as rigid template for the assembly of heterogeneous nanomaterials out of quantum dots and gold nanoparticles,[17] gold nanoparticle chiral tetramers,[11] gold

Received: November 18, 2014
Published: February 3, 2015

DOI: 10.1021/ph500434f
ACS Photonics 2015, 2, 392−397

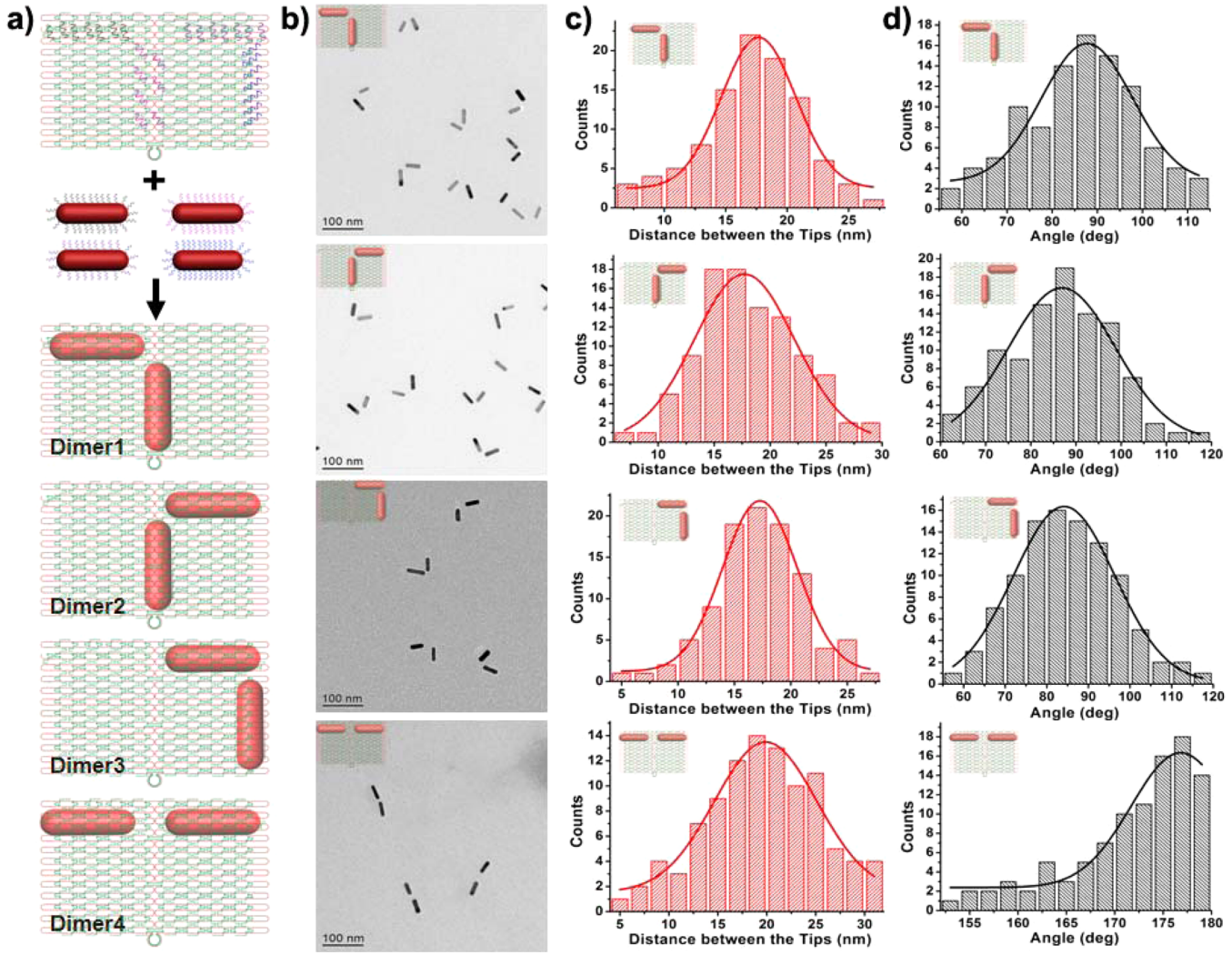

Figure 1. (a) Schematic illustration of the assembly of AuNRs onto the quasi-2D DNA origami forming AuNR dimer. When only considering the ideal design of AuNR structure without origami deformations, Dimers 1 and 2 can be viewed as reversed structures by flipping the origami plane around, which would be equivalent to a mirror reflection, thus, Dimers 1 and 2 are described as mirror-symmetric-like configurations here. (b) TEM images of the assembled AuNR dimers. (c, d) Statistics of the tip-to-tip distances and the angles between nanorods for different configurations.

nanorod dimer structures,[16,18] silver nanoparticle structures,[19] and self-similar gold nanoparticle chain structure.[20]

To our best knowledge, few studies have focused on significant impact of the nature of origami as soft materials on the property of the origami-guided nanostructures, in particular, the chiral nanostructures. In this work, we demonstrated that a series of AuNR dimer nanostructures, assembled on one side instead of two sides of a soft 2D DNA origami template, which was ideally taken as a 2D planar structures without chirality before,[21,22] can exhibit strong optical chiral responses. The flexibility of the soft DNA origami was found to play an essential role in the strong chiral response of the quasi-2D AuNR dimer nanostructures. The DNA origami templates (90 nm × 60 nm × 2 nm) were obtained by hybridizing a M13 single-stranded DNA (ssDNA) with a set of ~200 short staple strands[23] and were used to guide the assembly of AuNR dimer nanostructures (Figure 1a). First, AuNRs were functionalized with four different sets of ssDNA, respectively. Second, four types of capturing strands that are complementary to the ssDNA functionalized on AuNR surface protrude from one side of the DNA origami and seven copies of each capturing strand were used to anchor one AuNR on the DNA origami. Third, the predesigned AuNR dimer nanostructures were assembled by hybridizing the DNA origami and AuNRs. Four types of AuNR dimer nanostructures were designed and assembled in this study as defined as Dimer 1, Dimer 2, Dimer 3, and Dimer 4, in which the geometrical symmetry was finely tuned by rationally designing the position of AuNR on the origami. The assembled AuNR dimer nanostructures were collected by gel electrophoresis in a high purity up to 90% as manifested by transmission electron microscopy (TEM) images in Figure 1b (see Supporting Information for more TEM images). As shown in Figure 1c,d, most of the tip-to-tip distances are about 15−20 nm, and most of the angles for Dimer 1, Dimer 2, and Dimer 3 are about 80−95° and 170−180° for Dimer 4. These statistics further depict that all of the assembled configurations are in good agreement with our original design. It is notable that the observed objects under TEM slightly vary from the predesigned model structures, which resulted from the drying process during sampling.

We then carried out the plasmon absorption measurement of the purified Dimers. As exhibited in Figure 2a, both DNA-capped AuNRs and AuNR/origami monomer conjugates have

DOI: 10.1021/ph500434f
ACS Photonics 2015, 2, 392−397

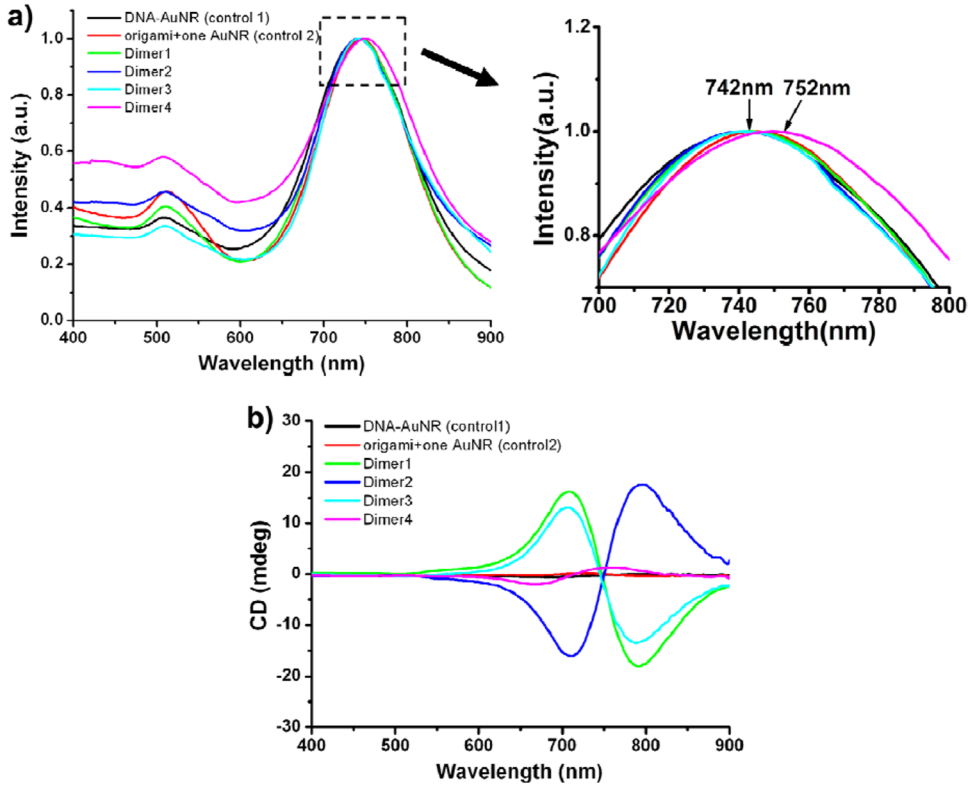

Figure 2. (a) Absorption and (b) circular dichroism spectra of the four types of AuNR dimers. The plasmonic chirality responds much more sensitively to the spatial variation of the assembled AuNR dimers, compared to their plasmon resonance coupling.

longitudinal plasmon resonance frequency close to 742 nm, illustrating the negligible influence of DNA sequences and DNA origami on the plasmon resonance property of AuNRs. Due to the weak interactions between the longitudinal plasmon modes, Dimers 1−3 with "L" geometry have close resonance peak position as compared with the AuNR/origami monomer conjugates. In contrast, when AuNRs are arranged along the length axis forming linear geometry, strong coupling occurs between the longitudinal plasmonic dipoles, giving rise to a large plasmon wavelength shift of 10 nm (Dimer 4 in Figure 2a). Such strong plasmonic interactions within the linear geometry of AuNR dimer were also reported on the single particle level.[24,25] Overall, the plasmon resonance frequency shifts insensitively with varying the configuration of Dimers. Especially, the "L" geometry shows almost the same plasmon resonance frequency in comparison with its mirror-symmetric-like counterpart. Therefore, it is difficult to identify the detailed structures and distinguish the conformations of these enantiomers by monitoring their plasmonic absorptions.

In spite of the "seemingly" 2D geometry, the L-assemblies exhibit strong optical activity, which can be clearly observed using circular dichroism (CD) spectroscopy. CD spectroscopy is widely used in the structural analysis of organic molecules and biomolecules, because the CD spectrum arises from the differential absorptions of left- and right-handed circularly polarized light for the molecular chiral center, and is very sensitive to the 3D arrangement of molecule dipoles. Metal nanoparticles have much larger optical absorption than small organic molecules because their surface plasmon resonances greatly increase the absorption cross-section, leading to the enhanced CD response at plasmonic resonance wavelengths. As illustrated in Figure 2b, single AuNR/origami (monomer) shows almost no CD signal, indicating that the chirality observed here is not mainly contributed by the molecular chirality of DNA origami. The asymmetric "L"-shaped assemblies of Dimers 1−3 present much higher CD signals around the longitudinal plasmon frequency compared to the linear geometry of Dimer 4. In particular, Dimers 1 and 2 exhibit reversed CD spectra arising from their mirror-symmetric-like configurations. Dimers 1 and 3 have close optical activities not only in handedness but also in CD signal intensity, as a result of their similar L-shaped configurations of AuNR arrangements.

In previous studies, DNA origami templates were widely considered as rigid, planar substrates for guiding the assembly of nanoparticles.[11,16−20] In that case, the as-assembled AuNR dimer structures templated by the 2D DNA origami would not exhibit chiroptical activities according to our numerical simulations (discussed below). However, as observed in Figure 2b, the "L" dimer assemblies obtained in our study exhibited significant CD signals. This means that the AuNR dimers are supposed to have certain 3D configurations. Further, these 3D "L"-shaped AuNR dimers are highly comparable to the plasmonic version of the Born-Kuhn modeled structures that can be realized as two identical corner-stacked and orthogonal nanorods. The near field plasmonic coupling between the nanorod resonantors generates bonding and antibonding plasmonic modes according to the hybridization model. These two plasmonic modes have differential absorption for the left- and right-handed circularly polarized light in different wavelength region, and thus give rise to the characteristic bisignate line shape of chiral spectra. Giessen et al. have also experimentally observed similar chiroptical activities from their plasmonic Born-Kuhn system consisting of two nanorods

DOI: 10.1021/ph500434f
ACS Photonics 2015, 2, 392−397

fabricated through a two-step electron beam lithography procedure.[26]

Now let us consider how the basic origami template induces 3D configurations of the assembled AuNR dimer structures, in the view of the original design of origami. According to the classic design of the origami used here, the DNA double helix in DNA origami (10.67 bp/turn) deviates from the natural B-type helical pitch (10.4 bp/turn). Such minimal structural difference can induce slight strain during the formation of the origami and cause the origami template to curve. As shown in Figure 3, we use Cando software to replot the DNA origami

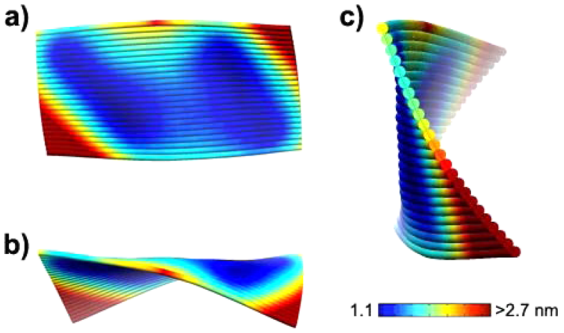

Figure 3. Replotted modeled origami structure from Cando software: (a) the front view, (b) the top view, (c) the side view.

template employed in this study, which undoubtedly depicts the curvature and 3D structure of the origami (see Supporting Information for details).[27] Such 3D configuration of the DNA origami template will propagate its 3D nature to the assembled AuNR dimers.

In addition to the curvature of the DNA origami, the intrinsic softness and dynamic motion of origami in solution also influence the real-conformation of the assembled AuNR structures, and such structural dynamics is hard monitored by TEM or cryo-TEM which are usually used to imaging static objects.[28] Nevertheless, we monitored the ensembles of origami-guided nanostructures through chiral signal output, which is highly sensitive to the in situ structure of the measured objects.

We have experimentally demonstrated the 3D native conformation of the AuNR dimer structures assembled on the classic planar origami template. To further disclose the real conformation of the AuNR dimer nanostructures, numerical simulations of the optical activities were carried out using Comsol Multiphysics based on the finite-element methods (see Supporting Information for details). Because the mirrored-symmetric like AuNR dimers display vertically symmetric chiral spectra, we choose single typical enantiomeric structure (Dimer 1) for the theoretical studies. The numerical method was first validated by comparing the simulated absorption spectrum of a single AuNR with the experimental result. Based on the AuNR dimension obtained statistically from TEM images (10 nm × 36 nm), the nanorods in simulation exhibited an absorption peak at 745 nm which agrees well with the experimentally measured resonance (Figure 4a). This peak is the longitudinal dipole resonance from the AuNR as confirmed by the simulated charge distribution image (inset in Figure 4a).

The single longitudinal peak splits into two peaks (728 and 763 nm) when such two AuNRs were placed close to each other (Figure 4a). By examining the simulated field distribution and the spatially resolved charge density (insets in Figure 4a),

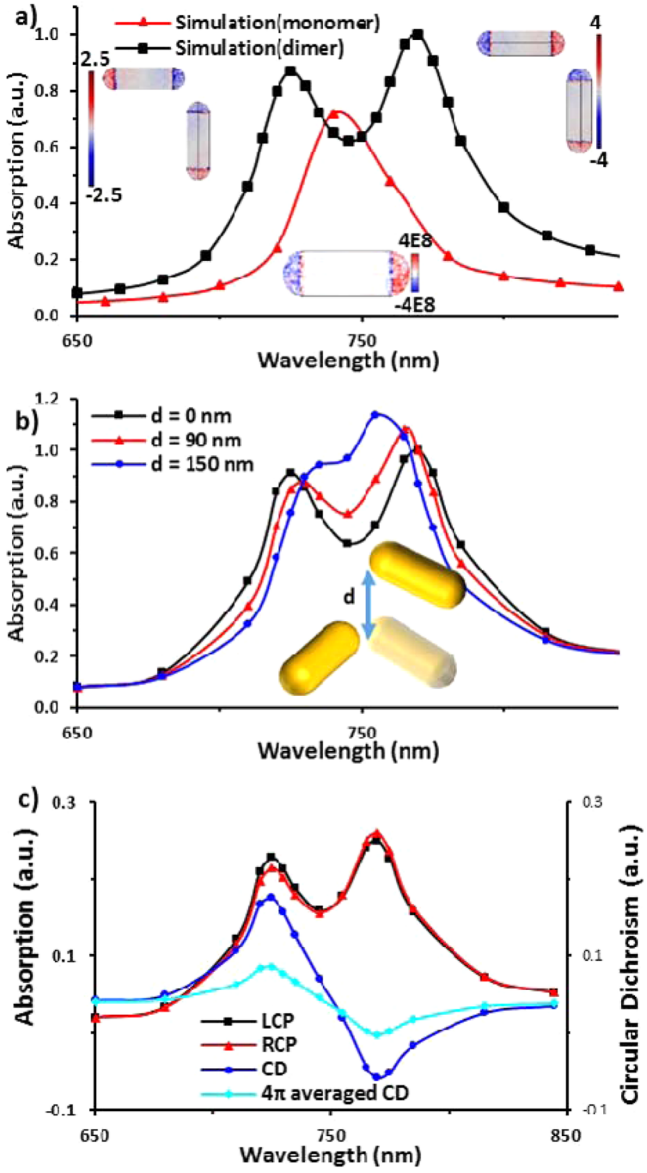

Figure 4. (a) Simulated absorption spectra of monomer (red triangles) and dimer (black squares) assemblies. The peak splitting due to the near-field coupling can be observed in the spectrum of the AuNR dimer. The insets are the charge density distribution of the AuNR assemblies showing the dipolar mode on each AuNR. (b) The spectral peak split between the bonding and antibonding resonances of AuNR dimer assemblies reduces with increasing inter-rod spacing, indicating weaker coupling at larger distance. (c) The amplitude of the split resonances changes in different directions as the illumination switches from left-hand circular polarization to right-hand polarization (black square and red triangle, respectively). Such opposite changes resulted in the CD with a positive amplitude at 728 nm and negative at 768 nm (blue circles). Qualitatively similar chiral behavior is retained in the CD spectrum averaged over the 4π angles (cyan diamonds).

we found that the dipole resonances are oscillating in-phase between the AuNRs at the longer wavelength, whereas out-of-phase resonances are observed around the blue-shifted peak. Such characteristic oscillation patterns identify the two split peaks as bonding and antibonding resonances due to the electromagnetic coupling between the two dipole resonances from each AuNR.[29−31] It is worth noting that the double peaks were not observed experimentally, which can be explained by

DOI: 10.1021/ph500434f
ACS Photonics 2015, 2, 392−397

the variations of geometries over many AuNR assemblies being measured simultaneously in bulk solution. In fact, the inter-rod gap dependent simulations revealed that slight increases of the distance between the AuNRs would reduce the amount of wavelength shifting and likely smeared double-peak feature in experimental data (Figure 4b).

A planar AuNR dimer assembly (with two AuNRs located in the same plane) does not exhibit optical activity in simulations, as we would expect from its nonchiral geometry. However, as soon as one of the AuNRs tipped up even for a small angle (10° in our simulations), CD response appeared in simulated differential absorption spectra. Experimentally, the orientation of the AuNRs attached to the origami templates would follow the small curving of the template due to the strain predicted in Figure 3. The small curving brings the AuNR out of the original plane and results in a 3D chiral structure in the AuNR dimer assemblies. Based on the field distribution map provided by the numerical methods, the amplitude of these two resonances (bonding and antibonding) is sensitive to the polarization of the excitation light only when the AuNR assembly has a chiral structure. Figure 4c showed the simulated results from a dimer assembly with 15 nm tip-to-tip spacing and with one of the AuNR tipped up for 10° (pivot at the end of the NR). This subtle geometry change effectively brings one AuNR out of the plane the other AuNR is residing in, which therefore results in the chiral structure and the optical activities. The bonding (in-phase) mode appears to be more pronounced under right-handed circular polarization than that under the left-handed polarization, whereas the antibonding mode decreases in amplitude (Figure 4c). The opposite change of the magnitude between the two modes led to well-defined CD response. The differential absorption spectrum (under left-handed and right-handed polarized light) crosses zero right around 745 nm, the wavelength in the middle between the two split resonances.

To resemble the experimental measurement conditions where AuNR assemblies were dispersed in solution with random orientations, we further simulated the CD spectra from the full 4π angular directions to account for the effect of illumination directions on the geometrically anisotropic AuNR assemblies. Specifically, we simulated CD spectra by varying the incident light directions (θ and φ with 10° interval) and took a surface-area-weighted average of all the obtained spectra. The sign of the chirality appeared to be insensitive to the illumination direction, whereas the amplitude fluctuates as the illumination direction changed (Figure 4c). The averaged CD spectra over the angles in simulation agree with measured results very well. Alternatively, when we mirror the structure assembly, the chirality changes its sign and become negative at shorter wavelength and positive at longer wavelength.

The amplitude of the chirality in simulation is dependent on the interplane spacing of the nanorods forming the chiral structure. Since such chiral structure could only be resulted from the distortion of the origami template, further quantitative study in the future may provide a convenient method to measure the curving of origami platelets in solution based on optical spectroscopy.

In summary, strong plasmonic chirality was observed from the quasi 2D AuNR dimer nanoarchitectures assembled on a soft 2D origami, which were associated with their geometric asymmetry.[31] The intensity of the chiral response of the obtained AuNR dimers was significantly dependent on the flexibility of the template. Our results show that the critical role of the DNA template on the precise conformation of the assembled nanostructures and the properties thereof, which should not be depreciated and may be taken advantage of in the design of self-assembly of nanostructures, particularly when optical activities are of interest.

■ ASSOCIATED CONTENT

Supporting Information

Experimental details, more TEM images, and DNA sequences. This material is available free of charge via the Internet at http://pubs.acs.org.

■ AUTHOR INFORMATION

Corresponding Authors

*E-mail: qbwang2008@sinano.ac.cn.
*E-mail: h-gao@physics.fsu.edu.
*E-mail: whni2012@sinano.ac.cn.

Author Contributions

‡These authors contributed equally to this work (Z.C., X.L., and Y.-C.C.).

Notes

The authors declare no competing financial interest.

■ ACKNOWLEDGMENTS

The authors acknowledge funding by Chinese Academy of Sciences "Strategic Priority Research Program" (Grant No. XDA01030200), the National Science Foundation of China (Grant No. 21303249, 21301187, 201425103), the National Science Foundation of Jiangsu province, China (Grant No. BK2012007), and the Chinese Ministry of Science and Technology (Grant No. 2011CB965004). H.G. and Y.-C.C. acknowledge the support from the Florida State University Start-up funds and the FSU FYAP Award.

■ REFERENCES

(1) Pendry, J. B. A Chiral Route to Negative Refraction. *Science* **2004**, *306*, 1353−1355.

(2) Zhang, S.; Park, Y. S.; Li, J. S.; Zhang, W. L.; Zhang, X. Negative Refractive Index in Chiral Metamaterials. *Phys. Rev. Lett.* **2009**, *102*, 023901.

(3) Gansel, J. K.; Thiel, M.; Rill, M. S.; Decker, M.; Bade, K.; Saile, V.; von Freymann, G.; Linden, S.; Wegener, M. Gold Helix Photonic Metamaterial as Broadband Circular Polarizer. *Science* **2009**, *305*, 1513−1515.

(4) Zhao, Y.; Belkin, M. A.; Alù, A. Twisted Optical Metamaterials for Planarized Ultrathinbroadband Circular Polarizers. *Nat. Commun.* **2012**, *3*, DOI: 10.1038/ncomms1877.

(5) Wu, X.; Xu, L.; Liu, L.; Ma, Wei.; Yin, H.; Kuang, H.; Wang, L.; Xu, C.; Kotov, N. A. Unexpected Chirality of Nanoparticle Dimers and Ultrasensitive Chiroplasmonic Bioanalysis. *J. Am. Chem. Soc.* **2013**, *135*, 18629−18636.

(6) Hendry, E.; Carpy, T.; Johnston, J.; Popland, M.; Mikhaylovskiy, R.; Lapthorn, A. J.; Kelly, S. M.; Barron, L. D.; Gadegaard, N.; Kadodwala, M. Ultrasensitive Detection and Characterization of Biomolecules using Superchiral Fields. *Nat. Nanotechnol.* **2010**, *5*, 783−787.

(7) Fan, Z.; Govorov, A. O. Plasmonic Circular Dichroism of Chiral Metal Nanoparticle Assemblies. *Nano Lett.* **2010**, *10*, 2580−2587.

(8) Hentschel, M.; Schäferling, M.; Weiss, T.; Liu, N.; Giessen, H. Three-Dimensional Chiral Plasmonic Oligomers. *Nano Lett.* **2012**, *12*, 2542−2547.

(9) Hentschel, M.; Wu, L.; Schäferling, M.; Bai, P.; Li, E. P.; Giessen, H. Optical Properties of Chiral Three-Dimensional Plasmonic Oligomers at the Onset of Charge-Transfer Plasmons. *ACS Nano* **2012**, *6*, 10355−10365.

DOI: 10.1021/ph500434f
ACS Photonics 2015, 2, 392−397

(10) Fan, Z.; Zhang, H.; Govorov, A. O. Optical Properties of Chiral Plasmonic Tetramers: Circular Dichroism and Multipole Effects. *J. Phys. Chem. C* **2013**, *117*, 14770−14777.
(11) Shen, X.; Asenjo-Garcia, A.; Liu, Q.; Jiang, Q.; García de Abajo, F. J.; Liu, N.; Ding, B. 3D Plasmonic Chiral Tetramers Assembled by DNA Origami. *Nano Lett.* **2013**, *13*, 2128−2133.
(12) Yan, W.; Xu, L.; Xu, C.; Ma, W.; Kuang, H.; Wang, L.; Kotov, N. A. Self-Assembly of Chiral Nanoparticle Pyramids with Strong R/S Optical Activity. *J. Am. Chem. Soc.* **2012**, *134*, 15114−15121.
(13) Valev, V. K.; Baumberg, J. J.; Sibilia, C.; Verbiest, T. Chirality and Chiroptical Effects in Plasmonic Nanostructures: Fundamentals, Recent Progress, and Outlook. *Adv. Mater.* **2013**, *25*, 2517−2534.
(14) Kuzyk, A.; Schreiber, R.; Fan, Z.; Pardatscher, G.; Roller, E.-M.; Högele, A.; Simmel, F. C.; Govorov, A. O.; Liedl, T. DNA-Based Self-Assembly of Chiral Plasmonic Nanostructures with Tailored Optical Response. *Nature* **2012**, *483*, 311−314.
(15) Dai, G.; Lu, X.; Chen, Z.; Meng, C.; Ni, W.; Wang, Q. DNA Origami-Directed, Discrete Three-Dimensional Plasmonic Tetrahedron Nanoarchitectures with Tailored Optical Chirality. *ACS Appl. Mater. Interfaces* **2014**, *6*, 5388−5392.
(16) Lan, X.; Chen, Z.; Dai, G.; Lu, X.; Ni, W.; Wang, Q. Bifacial DNA Origami-Directed Discrete, Three-Dimensional, Anisotropic Plasmonic Nanoarchitectures with Tailored Optical Chirality. *J. Am. Chem. Soc.* **2013**, *135*, 11441−11444.
(17) Wang, R.; Nuckolls, C.; Wind, S. J. Assembly of Heterogenous Functional Nanomaterials on DNA Origami Scaffolds. *Angew. Chem., Int. Ed.* **2012**, *51*, 11325−11327.
(18) Shen, X.; Zhan, P.; Kuzyk, A.; Liu, Q.; Asenjo-Garcia, A.; Zhang, H.; de Abajo, F. J. G.; Govorov, A.; Ding, B.; Liu, N. *Nanoscale* **2014**, *6*, 2077−2081.
(19) Pal, S.; Deng, Z.; Ding, B.; Yan, H.; Liu, Y. DNA Origami Directed Self-Assembly of Discrete Silver Nanoparticle Architectures. *Angew. Chem., Int. Ed.* **2010**, *49*, 2700−2704.
(20) Ding, B.; Deng, Z.; Yan, H.; Cabrini, S.; Zuckermann, R. N.; Bokor, J. Gold Nanoparticle Self-Similar Chain Structure Organized by DNA Origami. *J. Am. Chem. Soc.* **2010**, *132*, 3248−3249.
(21) Wang, D.; Capehart, S. L.; Pal, S.; Liu, M.; Zhang, L.; Schuck, P. J.; Liu, Y.; Yan, H.; Francis, M. B.; De Yoreo, J. J. Hierarchical Assembly of Plasmonic Nanostructures using Virus Capsid Scaffolds on DNA Origami Templates. *ACS Nano* **2014**, *8*, 7896−7904.
(22) Stephanopoulos, N.; Liu, M.; Tong, G. J.; Li, Z.; Liu, Y.; Yan, H.; Francis, M. B. Immobilization and One-Dimensional Arrangement of Virus Capsids with Nanoscale Precision Using DNA Origami. *Nano Lett.* **2010**, *10*, 2714−2720.
(23) Ke, Y.; Lindsay, S.; Chang, Y.; Liu, Y.; Yan, H. Self-Assembled Water-Soluble Nucleic Acid Probe Tiles for Label-Free RNA Detection. *Science* **2008**, *319*, 180−183.
(24) Tabor, C.; Van Haute, D.; El-Sayed, M. A. Effect of Orientation on Plasmonic Coupling between Gold Nanorods. *ACS Nano* **2009**, *3*, 3670−3678.
(25) Shao, L.; Woo, C. K.; Chen, H.; Jin, Z.; Wang, J.; Lin, H.-Q. Angle- and Energy-Resolved Plasmon Coupling in Gold Nanorod Dimers. *ACS Nano* **2010**, *4*, 3053−3062.
(26) Yin, X.; Schäferling, M.; Metzger, B.; Giessen, H. Interpreting Chiral Nanophotonic Spectra: the Plasmonic Born-Kuhn Model. *Nano Lett.* **2013**, *13*, 6238−6243.
(27) Kim, D.-N.; Kilchherr, F.; Dietz, H.; Bathe, M. *Nucleic Acids Res.* **2012**, *40*, 2862−2868.
(28) Bai, X.-C.; Martin, T. G.; Scheres, S. H. W.; Dietz, H. *Proc. Natl. Acad. Sci. U.S.A.* **2012**, *109*, 20012−20017.
(29) Nordlander, P.; Oubre, C.; Prodan, E.; Li, K.; Stockman, M. I. Plasmon Hybridization in Nanoparticle Dimers. *Nano Lett.* **2004**, *4*, 899−903.
(30) Willingham, B.; Brandl, D. W.; Nordlander, P. Plasmon Hybridization in Nanorod Dimers. *Appl. Phys. B: Laser Opt.* **2008**, *93*, 209−216.
(31) Funston, A. M.; Novo, C.; Davis, T. J.; Mulvaney, P. Plasmon Coupling of Gold Nanorods at Short Distances and in Different Geometries. *Nano Lett.* **2009**, *9*, 1651−1658.

DOI: 10.1021/ph500434f
ACS Photonics 2015, 2, 392−397